



Expression and sequences of genes encoding glutamate receptors and transporters in primate retina determined using 3'-end amplification polymerase chain reaction

Michael C. Hanna,^{1,2} David J. Calkins³

¹Interdisciplinary Program in Neuroscience, The University of Rochester Medical Center, Rochester, NY; ²The National Institute of Neurological Disorders and Stroke, National Institutes of Health, Cellular Neurology Unit, Bethesda, MD; ³The Vanderbilt Eye Institute, Department of Ophthalmology and Visual Sciences, Vanderbilt University Medical Center, Nashville, TN

Purpose: Our long-term goal is to compare how expression of glutamate receptor and non-vesicular transporter subunits differs between single neurons in the primate retina. Here we set out to ascertain general expression in the retina of *Macaca fascicularis* using a robust technique suitable for both levels of analysis. We constructed full-complement cDNAs from whole retina RNA using a protocol optimized for detection of even low-abundance transcripts and for transcripts of various lengths. We probed these libraries for expression of genes encoding the AMPA- (GluR1-4) and kainate-sensitive (GluR5-7, KA1-2) ionotropic glutamate receptors, the metabotropic glutamate receptors (mGluR1-8), and five non-vesicular glutamate transporters (EAAT1-5) in the macaque retina and brain and determined large portions of coding sequences for each. We also asked whether each gene can be detected in cDNA generated from a limited amount of RNA extracted from an aldehyde-fixed retinal slice, a technique useful for probing gene expression in tissue used for histological studies.

Methods: We constructed full-length cDNA from RNA harvested from the macaque retina using a modified version of the 3'-end amplification (TPEA) technique of Dixon et al. [1]. With this technique, the 3' region is amplified arbitrarily using multiple primers to produce amplified cDNA containing as diverse and complete sample of genes as possible. We probed the cDNA for expression of glutamate receptors and non-vesicular transporters using gene-specific RT-PCR and assembled sequences from the reaction products using a series of overlapping primer pairs. We also used TPEA to compare expression in a small amount of RNA extracted from a fixed retinal slice.

Results: Macaque retinal cDNA created using TPEA contains a high abundance of transcripts of various lengths. Gene-specific PCR using primers designed against human sequences indicates expression for all GluR, mGluR, and non-vesicular transporter subunits for which we probed. Expression patterns were similar between two different macaque retinas, but different in brain. Several differences also exist between macaque and human brain. For some subunits, this is the first demonstration of expression in the macaque retina. The expression pattern obtained probing cDNA libraries generated from fixed tissue RNA with a different primer set was similar to that for fresh tissue. We sequenced between 1865 (mGluR8a) and 3697 (mGluR1) total nucleotides for each macaque gene and obtained complete coding sequences for GluR1-7, mGluR3 and mGluR4. A comparison with the corresponding human sequences reveal that the coding region of macaque GluR6 demonstrates the highest homology with only 26 nucleotide substitutions (99% homology), while mGluR4 demonstrates the lowest with 68 substitutions (97.5%).

Conclusions: Neural tissue cDNA created using TPEA contains diverse transcripts of varying size, abundance, and homology. We established using TPEA the expression of all nine AMPA- and kainate-sensitive GluRs, all eight mGluRs and all five non-vesicular glutamate transporters and found that expression differs between macaque retina, macaque brain and human brain. The nucleotide sequences for the coding regions differed moderately between the human and macaque genes. We also found a similar expression pattern in a smaller amount of RNA extracted from a fixed retinal slice. Thus, this technique could be useful for comparing gene expression in cells extracted from fixed tissue pre-labeled using specific markers.

The transfer of visual information through the retina is mediated by the tonic release of glutamate at two levels of excitatory, feed-forward connections. In the outer retina, at the photoreceptor synapse, glutamate binds to receptors localized to the processes of inhibitory horizontal cells and the

dendrites of excitatory bipolar cells. In the inner retina, at the bipolar cell axon terminal, released glutamate binds receptors on processes of amacrine cells (mostly inhibitory) and the dendrites of ganglion cells, whose axons comprise the optic nerve [2,3]. This fundamental design is highly conserved across mammalian species. However, a great deal of functional specialization that is species-dependent is imparted to the various neuronal cell types through their synaptic connections with one another and through their pharmacological properties. Functional diversity between cell types within the glutamatergic feed-forward pathway is due in large part to

Correspondence to: Dr. David Calkins, The Vanderbilt Eye Institute, Department of Ophthalmology and Visual Sciences, Vanderbilt University Medical Center, 8000 Medical Center East, Nashville, TN 37232; Phone: (615) 936-6412; FAX: (615) 936-6410; email: david.j.calkins@vanderbilt.edu

differential expression of multiple types of ligand-gated or ionotropic glutamate receptors (GluR) and G-protein coupled metabotropic glutamate receptors (mGluR). The GluRs are integral membrane proteins that gate nonselective cation channels upon binding glutamate. These comprise three major classes based on their affinity for particular agonists: N-methyl-D-aspartate (NMDA), (α -amino-3-hydroxy-5-methyl-4-isoxazolepropionic acid [AMPA]), or kainate (KA). The GluRs are tetrameric complexes assembled from two or more structurally similar subunits drawn from either a single gene family (AMPA: GluRs 1-4), two gene families (kainate: GluRs 5-7 and KAs 1-2), or three gene families (NMDA: NR1, NR2A-D, NR3A-B) [4]. The mGluRs couple to GTP-binding proteins and activate various second messenger systems to induce a large array of cellular effects. To date, eight homologous subtypes (mGluR1-8) and some splice variants have been cloned [5,6].

The regulation of extracellular glutamate by non-vesicular glutamate transporters is of particular importance in the retina, where glutamate is released tonically from the photoreceptor axon terminal and can reach concentrations that would be potentially toxic to a numerous other neurons [7]. Such regulation is also necessary to maintain a high signal-to-noise ratio for transmission and to help shape post-synaptic responses. The five major isoforms of non-vesicular glutamate transporters are EAAT1 (GLAST), EAAT2 (GLT-1), EAAT3 (EAAC1), EAAT4, and EAAT5. Numerous immunocytochemical studies across species have established general patterns of localization that lend a great deal of insight into the functional significance of the GluRs, mGluRs, and EAATs [8-21]. Even with burgeoning information about the localization and physiological role of glutamate receptors and transporters in the retina, only a limited amount of information exists about the patterns of expression for the genes encoding these receptors and transporters [8,19,22-26]. Genetic profiling of the mammalian retina thus far focuses primarily on rodent [27-31], with very little information for primate species, including *macaca*, the traditional animal model for human vision. Such information is critical for drawing functional conclusions about retinal circuits based on genetic and molecular profiling.

Our long-term goal is to link patterns of gene expression involved in glutamatergic signaling with particular morphological cell types in the primate retina [32]. However, first we required a robust technique to construct full-complement cDNA from the retina of *Macaca fascicularis* suitable for amplification of even low-abundance transcripts, for transcripts of various lengths, and transcripts with high similarity. To this end, we applied a modified version of 3'-end amplification (TPEA) RT-PCR [1] to construct full-length libraries and then probed these libraries using gene-specific PCR. We determined from this cDNA the expression and the sequences for genes encoding specific glutamate receptors and transporters using gene-specific PCR. Here we report the expression of GluR1-7, KA1-2, mGluR1-8, and EAAT1-5. After confirming the specificity of our PCR products, we constructed full-length sequences for the genes encoding GluR1-6, mGluR3, and

mGluR4, as well as large portions of the remaining receptors and transporters. We also demonstrate that this powerful technique is also suitable for small amounts of RNA extracted from fixed tissue.

METHODS

Animals and tissue preparation: We obtained fresh retina from an eye of each of two adult *Macaca fascicularis* used in unrelated studies in adherence with federal guidelines and institutional policy. Following euthanasia, isolated eyecups were cleaned of vitreous and the retinas dissected free and homogenized in TRIzol Reagent (1 ml/100 mg tissue; Life Technologies, Rockville, MD) with subsequent RNA isolation according to manufacturer's instructions. The RNA was treated with DNase I (Invitrogen, Carlsbad, CA; 10 U/ μ l) at 37 °C for 30 min prior to reverse transcription and subsequent PCR to avoid DNA contamination. The pure RNA was phenol chloroform extracted to remove any residual DNase and resuspended in DEPC-treated water to a final concentration of about 1.00 mg/ml, determined spectrophotometrically for each sample. We also obtained samples of cerebral cortex from a single *Macaca fascicularis* (Yerkes Regional Primate Research Center, Atlanta, GA). These were removed fresh, flash-frozen on dry ice for shipment, and processed using the same protocol we applied to the retina. Human brain total RNA was purchased from Ambion, Inc. (Austin, TX).

For cDNA construction from RNA extracted from fixed tissue, a macaque retina was immediately immersion-fixed in 4% paraformaldehyde for two hrs. The retina was then washed extensively in 0.01 M PBS, embedded in 5% agar and cut into 40-60 μ m thick vertical sections on a vibratome. RNA extraction was as previously described [33]. Briefly, under RNase-free conditions, each vertical section was resuspended in 200 ml of RNA extraction buffer containing 10 mM Tris/HCl, pH 8.0; 0.1 mM EDTA (ethylenediamine-tetraacetic acid), pH 8.0; 2% SDS (sodium dodecyl sulfate, pH 7.3; and 500 mg/ml Proteinase K, Ambion Inc., Austin, TX) and incubated at 60 °C for 16 h until the tissue was completely solubilized. After Proteinase K treatment, the cellular components were digested with DNase I (Invitrogen, 10 U/ μ l) at 37 °C for 30 min to avoid DNA contamination. RNA was purified by phenol chloroform extraction (equal volume) followed by precipitation with an equal volume of isopropanol in the presence of 0.1 volume of 3 M sodium acetate (pH 4.0), and 1 ml of 20 mg/ml glycogen, which acts as an RNA carrier, at -20 °C. The resulting RNA pellets were washed in 70% ethanol, centrifuged for 5 min at 4 °C, allowed to dry and re-suspended in diethylpyrocarbonate (DEPC) -treated water to a final concentration -1.00 mg/ml, determined spectrophotometrically for each sample. Extracted RNA from each vertical section was used for TPEA-PCR and gene specific PCR (below).

cDNA construction: We followed a modification of the 3'-end amplification technique of Dixon et al. [1]. In this method, the 3' region of extracted mRNA is amplified arbitrarily by PCR using a combination of primers, so the amplified cDNA represents as diverse and complete sample of gene sequences as possible. Specific sequences are then amplified

with a second round of PCR using gene-specific primers. This technique is advantageous because it allows one to consistently amplify cDNA from very little mRNA, if necessary (as in the case for single cells), and to examine a broad range of genes.

For first strand synthesis, 1 µg of total retinal or brain mRNA was reverse-transcribed in 20 µl containing 1x first strand buffer, 200 U of Superscript® II reverse transcriptase

(Gibco, Grand Island, NY), 10 mM dNTPs (Gibco-BRL Grand Island, NY), 2 U of RNase OUT (Gibco-BRL Grand Island, NY), and an anchored oligo (dT) primer with a specific 5' heel sequence: CTC TCA AGG ATC TTA CCG CTT TTT TTT TTT TTT V (where V=A, C or G), for 60 min at 42 °C. We performed second strand synthesis using a combination of primers which contained (5' to 3') a different 20-mer heel sequence, and a stretch of five random nucleotides (CTG CAT CTA TCT AAT GCT CCN NNN N where N=A or C or T or G). In addition, each second-strand primer contained a defined pentameric sequence at the 3' end; these four arbitrary sequences were CGAGA, CGACA, CGTAC, and ATGCG. One ng of the primer mixture was annealed to the first-strand

TABLE 1. PRIMER SETS AGAINST HUMAN SEQUENCES USED IN FRESH-TISSUE PCR

Gene	Accession number	Location	Human sequence (5'-3')	Size (bp)
GluR1	NM_000827	1870 2371	F: AGACAACCAAGTACCAATG R: GAATCCAAGTACCTCCACCTTC	502
GluR2	NM_000826	1812 2314	F: TTTTTCCTACATTGGGGTCCAG R: TTTGGACTTCCGCACTCTAGCCAC	503
GluR3	NM_000828	1967 2467	F: TTGGAGTCAGCGTAGTTCTTTTCC R: TTCCCTTGGACTTTCGCACTCG	501
GluR4	NM_000829	1723 2222	F: ACAGAAGAGCCAGAGGACGGAAAG R: TCACATGGCTTTCGCTGCTA	500
GluR5	NM_000830	1776 2270	F: CCACCATTCCTGGAAGAACCCTATG R: TGTTTCCACCACGCTCTGAGTCAG	495
GluR6	NM_021956	2260 2715	F: CAGATTGGCGCCTTATAGACTC R: TTCTTTACCTGGCAACCTTCTGTCT	456
GluR7	NM_000831	2282 2760	F: AGATTGGGGGACTCATTGACTC R: TAAGGATGTGCTGCAGCCCATG	479
KA1	NM_014619	2041 2524	F: AATTCCTCCCTACAGACCTACC R: AGACGGACACCTCAGTTGCTTC	484
KA2	NM_002088	1287 1771	F: GTGGTCACAACCATCCTGGAGAAC R: AGGCATGGGTGTGGGTATATAC	485
mGluR1	NM_000838	1824 2316	F: AGGGCCAGATTAAAGTTATACGG R: CAGATCTTCTTCTGCTGCCAGC	493
mGluR2	NM_000839	1845 2333	F: CTCTGCTACTGCATGACCTTCATC R: CAGGAATGCCAGCCAGATGATG	489
mGluR3	NM_000840	1703 2215	F: GTCACTGGGCAGAAACCTTATCG R: AGATAGCGAAGGAACCTCCACG	513
mGluR4	NM_000841	1983 2468	F: GTGGTGATCACCTTTGTGCGCTAC R: TGTGACCATGAGCAGCATACTG	486
mGluR5	NM_000842	3738 4457	F: CCCCCTGTTCCACACACACAATG R: GCCTCCGTAATACTGGACCCAAAG	520
mGluR6	NM_000843	2675 3159	F: CGGCATGCTCTACGTACCCAAAAC R: AATCTCCCGCAAACCAAGGCAAAGC	485
mGluR7	NM_000844	2281 2763	F: CACTTTCATCCGCTACAATGACAC R: CCGAGTCTTGATGGCATAACAG	483
mGluR8	NM_000845	1450 1935	F: GGAGATGCTCCTGGACGTTATG R: TAGGAGCACGTAACCTAAGTTCCGG	486
EAAT1 (GLAST)	NM_004172	819 1025	F: TAAACAATGTGTCTGAGGCCATGG R: CTACCAGTCTCATGATGGCTTCG	207
EAAT2 (GLT-1)	NM_004171	1256 1446	F: TTCATTGCTTTTGGCATCGC R: TGCCTAGCAACCACTTCTAAGTCC	191
EAAT3 (EAAC-1)	NM_004170	808 995	F: ATTCAGATGGCATAAACCTGCTGG R: CCGAGCAATCAGGAACAAAATACC	188
EAAT4	NM_005071	706 907	F: GAACCAGCTTCCTGGAAAATGTC R: TTGAGGCTGTGGAAGAAGTCCCTG	202
EAAT5	NM_006671	877 1084	F: TCAGCTTCTGCCAGTGCCTCAATG R: TAGAGCAGGGGCAGGATAAAGAGC	208

“Accession number” represents GenBank accession number for the corresponding human gene. “Location” represents position of initial nucleotide for forward and reverse primer pairs. “Human sequence” represents sequence for design of forward and reverse primers. “Size” represents number of base pairs in expected PCR product.

TABLE 2. PRIMER SETS AGAINST HUMAN SEQUENCES USED IN FIXED-SLICE PCR

Gene	Accession number	Location	Human sequence (5'-3')	Size (bp)
GluR1	NM_000827	2071 2258	F: TGGTGTCTCCCAATTGAGAGTGC R: AATCATCCCTCCTCTGTGGTTC	188
GluR2	NM_000826	1559 1742	F: TTTTTCCTACATTGGGGTCCAG R: TAGTCTCTGGTTTCTCTGGGTGC	184
GluR3	NM_000828	2072 2262	F: CAGACTGAAATTCATATGGGACC R: TCCAGCAGGAAGGCAAACTTTC	191
GluR4	NM_000829	2068 2253	F: TGAAAAGATGTGACCTACATGCG R: GAATCCAGATTTCTCCCACTTTC	186
GluR5	NM_000830	2428 2631	F: TCTGGCTGCCTTCTTGACAGTAG R: TCACGTGTTCTTACCAGGCGGG	204
GluR6	NM_021956	1977 2182	F: GACAGTGGAAACGCATGGAATCC R: CTCGCTGGATTCTCTTCTCATTAC	206
GluR7	NM_000831	2153 2384	F: CTGATGACCTGGCCAAAGCAAC R: TTCCTCTGCGTGACGACTCGATG	232
KA1	NM_014619	2218 2433	F: GGGAAATGCCAGGGTGTGAATCC R: TTCAGGATCTCCAGGCGGTTGTTTC	216
KA2	NM_002088	2194 2398	F: CTCAACTGCAACCTCACCCAGATC R: CCAAACCTTTAGCTCGATGGTCC	205
mGluR1	NM_000838	2900 3085	F: AATGGCAAGTCTGTGTCATGGTC R: GCTGGTATCTGAAAAGGTCAGGC	186
mGluR2	NM_000839	2043 2241	F: CCATCTGCCTGGCATTATCTC R: AAGGCATAAAGCGTGCAGAGC	199
mGluR3	NM_000840	2047 2232	F: ATCAAGCACAACAACACACCCCTTG R: CAGCAGGCTGAGTAACAGATAGC	186
mGluR4	NM_000841	2683 2881	F: ACATGCCAAAAGTCTACATCATCC R: TAAGTCTGTTTGGTGGCCAGCG	199
mGluR5	NM_000842	2019 2223	F: TGGCATCTGCCTGGGCTACTTATG R: ACAGGCACTCATGCCTCTGGGC	205
mGluR6	NM_000843	2302 2491	F: AGGTGGTGGGATGATAGCATG R: TTGATGGGCTACACTGTGCACCG	190
mGluR7	NM_000844	2005 2229	F: CTGGGCTGTGATTCCTGTCTTC R: AAGCCCAAGAAAACCTCGCCG	225
mGluR8	NM_000845	2001 2181	F: CTCCTTCCGACGGGTCTCCCTA R: AAGGAGCTGGACGGAGATGA	181

The primers were used to detect genes from mRNA extracted from fixed retinal slices. The primers used to detect the glutamate transporters (EAAT1 through EAAT5) are the same used in fresh retinal tissue and are listed in Table 3. “Accession number” represents GenBank accession number for the corresponding human gene. “Location” represents position of initial nucleotide for forward and reverse primer pairs. “Human sequence” represents sequence for design of forward and reverse primers. “Size” represents number of base pairs in expected PCR product.

cDNA for 15 min at 50 °C using a PCR-Express thermal cycler (Hybaid, Waltham, MA.) to ramp and control all reaction temperatures. The second-strand synthesis was performed at 72 °C for 10 min using ThemalAce DNA polymerase (Invitrogen) according to manufacturer's instructions. To begin cDNA amplification, we subjected cDNA to 10 cycles consisting of 92 °C for 2.5 min, 60 °C for 1.5 min, and 72 °C for 1 min. This was followed by a 10 min extension at 72 °C, after addition of 0.5 ng of 3' heel primer (CTC TCA AGG ATC TTA CCG CTT). We then added 125 ng of second strand primers and 50 ng of 3' heel primer along with 47.5 ml of PCR reaction mix and further amplified the cDNA for 15 cycles with the same cycling parameters as before.

Following cDNA amplification, the concentration of the product for each tissue was determined with a spectrophotometer to ensure that equal amounts of cDNA were used for

gene-specific PCR. For negative controls, we used human brain RNA processed as described above but omitting the reverse transcriptase. The concentration of samples for negative controls was also measured because unincorporated dNTPs could still register on the spectrophotometer.

Gene-specific reverse transcriptase polymerase chain reaction: For gene-specific PCR, we designed primers to target unique regions of known human sequences accessed from GenBank using the sequence alignment feature of Vector NTI Suite 7.1 (InforMax, Inc., San Francisco, CA; Table 1, Table 2). These primer pairs were designed to generate products of either 450-600 base-pair regions for gene-specific PCR in fresh tissue or 180-220 base-pair regions for gene-specific PCR in fixed tissue. The uniqueness of each target sequence was confirmed with BLAST searches against all other known GenBank sequences using the National Center for Biotechnology Infor-

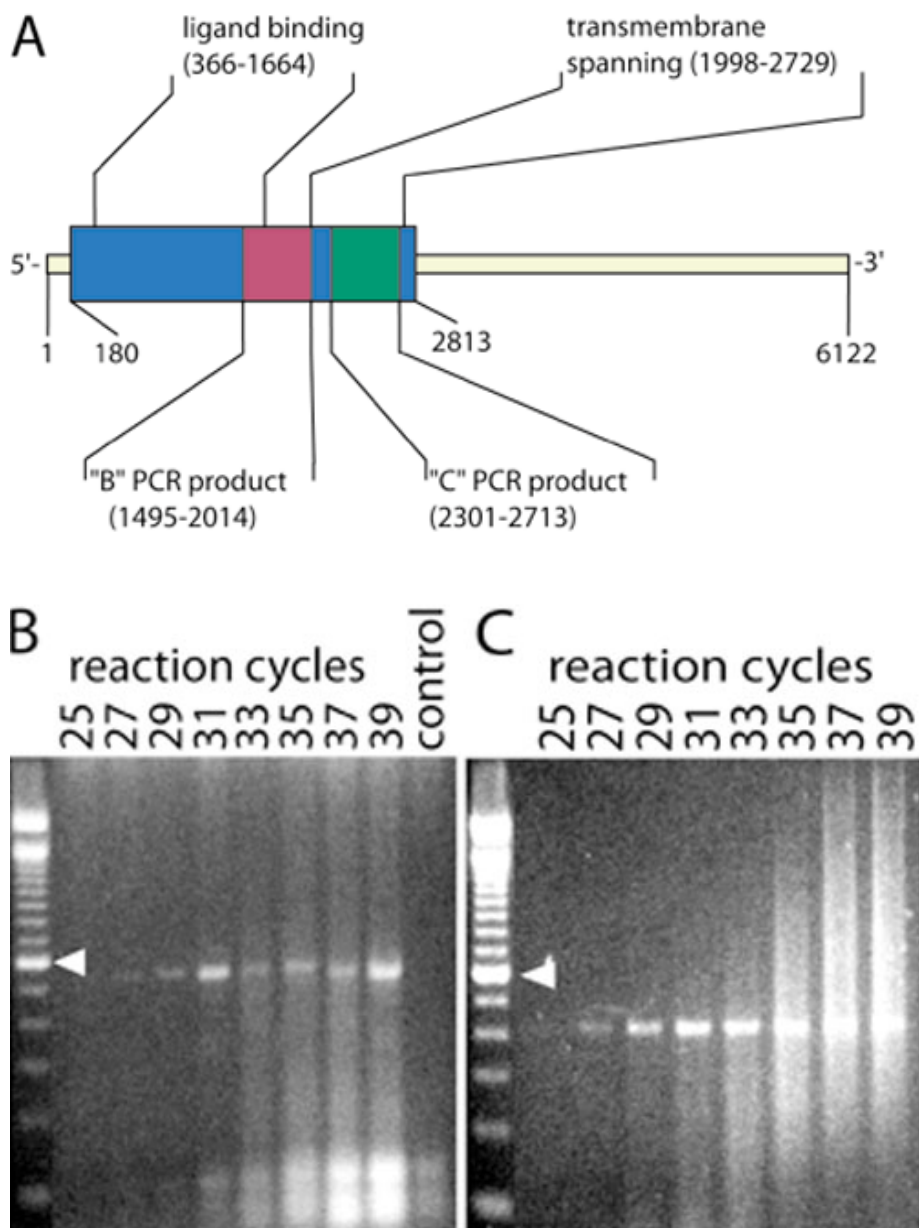


Figure 1. Sequence and expression of mGluR6 mRNA in primate retina. **A:** Schematic of gene encoding mGluR6 (6122 base pairs, Genbank NM_000843), indicating the coding region (blue area) and ligand-binding and transmembrane-spanning regions. Red and green areas represents highly specific regions targeted for PCR probing. **B:** Gene-specific PCR to detect mGluR6 within retinal cDNA library created using TPEA RT-PCR. The decrease in PCR product at 33 to 35 cycles is likely due to increased primer dimerization, indicated by the smears at the bottom of the gel. No mGluR6 mRNA is detected when reverse transcriptase is absent (control lane). Gene-specific primers were designed to produce a PCR product of 520 base pairs: 5'-GGA TGC TTC TGC AGT ACA TTC GAG-3' (sense) and 5'-TTG TTG TGT CGC ATG AAG GTG GCC-3' (antisense). **C:** Second gel demonstrating linear range for detection of mGluR6 using primers designed against a smaller segment of the coding region. Gene-specific primers were designed to produce a PCR product of 413 base pairs: 5'-CAG GTG GTG GGG ATG ATA GCA TG-3' (sense) and 5'-AAG AGG ATG ACG TAG GTT TTG GG-3' (antisense). In this case, there is less dimerization and the PCR product increases as expected with increasing number of cycles. Arrowhead again indicates 600 base pairs.

mation (NCBI) website. For each tissue sample, we added an equal amount (2 mg/ml) of cDNA to 50 µl of standard reaction mixture and 300 ng of gene-specific primers. Samples of the PCR products were loaded in equal amounts (5 µl) and separated on a 2% agarose gel containing ethidium bromide (0.5 µg/ml).

Identification sequencing: To confirm the selectivity of our primers, we precipitated representative PCR products for each glutamate receptor following phenol/chloroform extraction. Following centrifugation, the pellets were washed, air dried and resuspended in 5 µl Tris-EDTA buffer. Each suspension was run on a 1% low melt agarose gel, and each resulting band of DNA excised and purified using the Qiaex II Gel Extraction Kit (Qiagen Inc., Valencia CA). Following quantification with a DNA mass ladder, we sequenced the DNA (10 ng) using the original amplification primers in conjunction with the BigDye terminator kit (Perkin Elmer, Inc., Boston, MA). Samples of the precipitated reaction were run on a 3100 Automated Sequencer (Applied Biosystems, Inc., Foster City, CA) at the Nucleic Acid Core Facility at the University of Rochester. Sequence data was viewed and saved as a

FASTA file using Vector NTI 7.1 and identity confirmed using BLASTn program. Sequences had to match with perfect probability to a human mRNA or cDNA accession for acceptance.

Assembly of full-length sequences for macaca: For each gene, we combined the newly confirmed sequence obtained with the set of initial primers (Table 1) with the original human sequence to produce a subsequent series of highly efficient primer pairs (one human, one macaque). Each new primer pair generated a PCR product of approximately 500 base pairs that overlapped the preceding sequence by at least 100 base pairs at the 5' and 3' ends. Each series of primers was designed to produce a contiguous sequence with triplicate coverage of every portion of the gene. When positive, the PCR product from monkey retina was concentrated, excised and purified from the gel, and sequenced as described above. This process was repeated to assemble step-wise the full-length coding sequences using the Contig Express component of Vector NTI. To ensure that the entire start-to-stop region was sequenced, we attempted for each gene to continue the primer series until significant portions of both 5' and 3' untranslated regions were

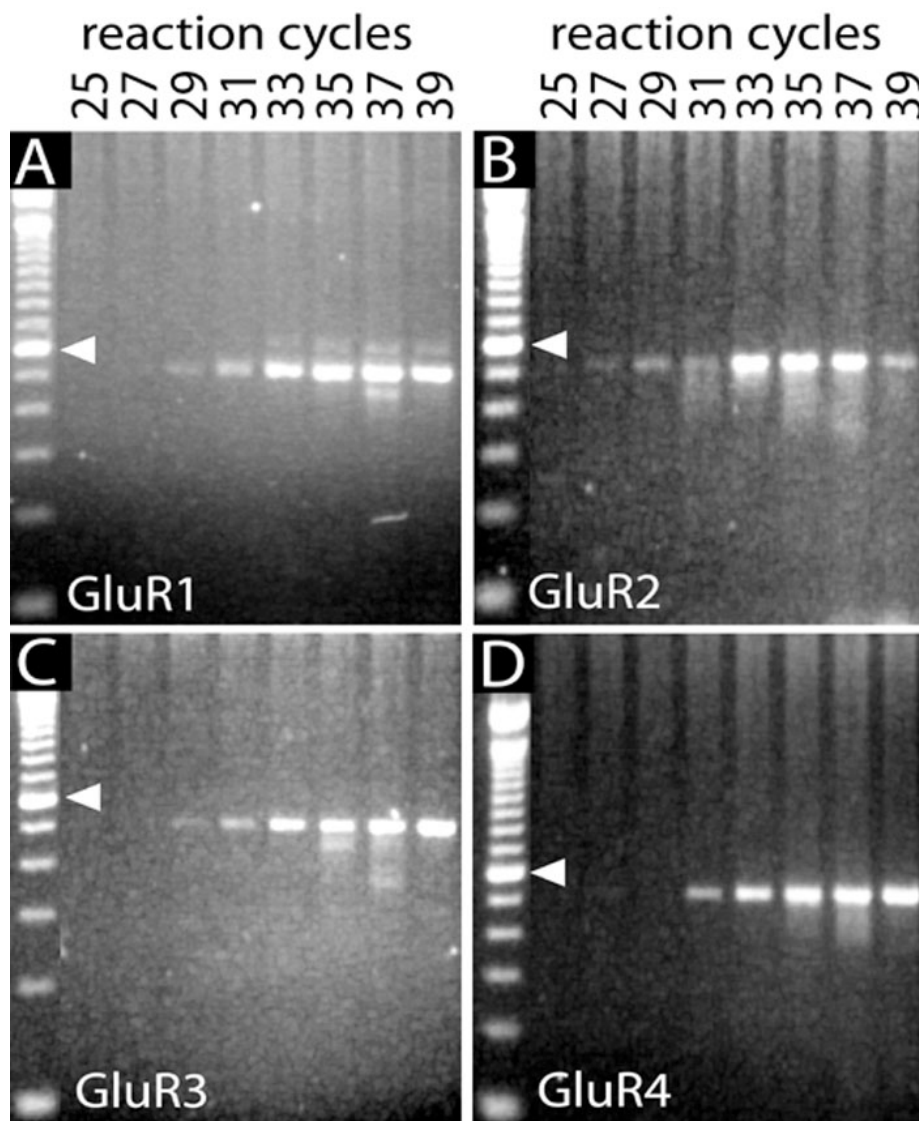


Figure 2. Expression of AMPA receptor genes in primate retina. Detection of AMPA subunits GluR1 (A), GluR2 (B), GluR3 (C) and GluR4 (D) using TPEA RT-PCR as described in Methods. As in the case of mGluR6 (Figure 1), the detection of each gene remains linear over a large range of PCR reaction cycles. No AMPA receptor mRNAs were detected when reverse transcriptase was omitted (data not shown). Arrowheads indicate 600 base pairs. Primers used for gene-specific PCR and expected product sizes are listed in Table 1.

included. This was not possible for certain genes where the untranslated regions of the human sequence are not listed in GenBank. For each series of primers, we also probed macaque brain and human brain cDNA for comparison. When full-length genes were determined, we compared the homology between the coding regions of the human and macaque using the AlignX component of Vector NTI. The sequence of genes for which the full length was not determined also was aligned to the

corresponding region of the human sequence. The direct strand sequence was translated to produce a predicted amino acid sequence, which was compared to the human to determine homology.

RESULTS

Construction and detection of large cDNAs: Our initial concern in creating an amplified cDNA library using TPEA RT-PCR was whether larger genes with coding region displaced substantially from the non-coding poly-A tail would be amplified. Theoretically, with TPEA RT-PCR, it is possible that such genes would not amplify since the poly-T primer used during the cDNA synthesis is designed to anneal to the poly-A tail and subsequent amplification reads inward from the 3'-end of the poly-T primer. To address this concern, we probed the cDNA library using gene-specific PCR with primers designed to the metabotropic subunit mGluR6, whose expression pattern across mammalian species is well-established [34,35]. We chose the gene for mGluR6 also because it has a relatively long 3' untranslated region as compared to other glutamate receptors. Figure 1A illustrates the coding region of the mGluR6 gene and the regions amplified during two independent sets of gene-specific PCR. This diagram illustrates that the length of the untranslated region from the poly-A tail to the stop codon is 3309 base pairs (base pair loci 6122-2813) and the distance to the 5'-end of the forward gene-specific primer is 4627 base pairs (6122-1495). Nevertheless, we are still able to amplify mGluR6 and detect the full 519 and 412 base-pair products using gene-specific PCR beginning around 27 reaction cycles (Figure 1B-C). Moreover, the detection of mGluR6 with gene-specific PCR remains approximately linear over a wide range of reaction cycles, despite pre-amplification of the whole-retina cDNA. This implies that the initial construction and amplification of cDNA with TPEA is not so extreme that gene-specific PCR is immediately non-linear, thus highly expressed genes such as mGluR6 may not be preferentially amplified.

Detection of glutamate receptors and transporters in retina and brain: With TPEA, the primers used during cDNA amplification necessarily recognize a common region of genes. Therefore we were also concerned that in the synthesis of cDNA, similar genes may not amplify equally. It is possible that only the most abundant genes could amplify at the expense of amplification of genes of lower expression. To test whether we could use TPEA to detect similar genes from a single pool of RNA, we utilized the same cDNA library used to detect mGluR6 (Figure 1) to compare four highly homologous genes over a considerable range of reaction cycles. Figure 2 demonstrates detection of the mRNAs encoding the AMPA receptor subunits GluR1-4 over the same range of PCR cycles used to detect mGluR6. Each gene is detectable as early as 31 cycles and seems to have a roughly equivalent amplification rate. Similar to mGluR6, the amplification of each gene remains in its linear range over a significant number of cycles, but appears to peak around 35 cycles. Therefore, all subsequent gene-specific PCR reactions utilized 35 cycles, and the PCR product from each was sequenced to confirm gene-spe-

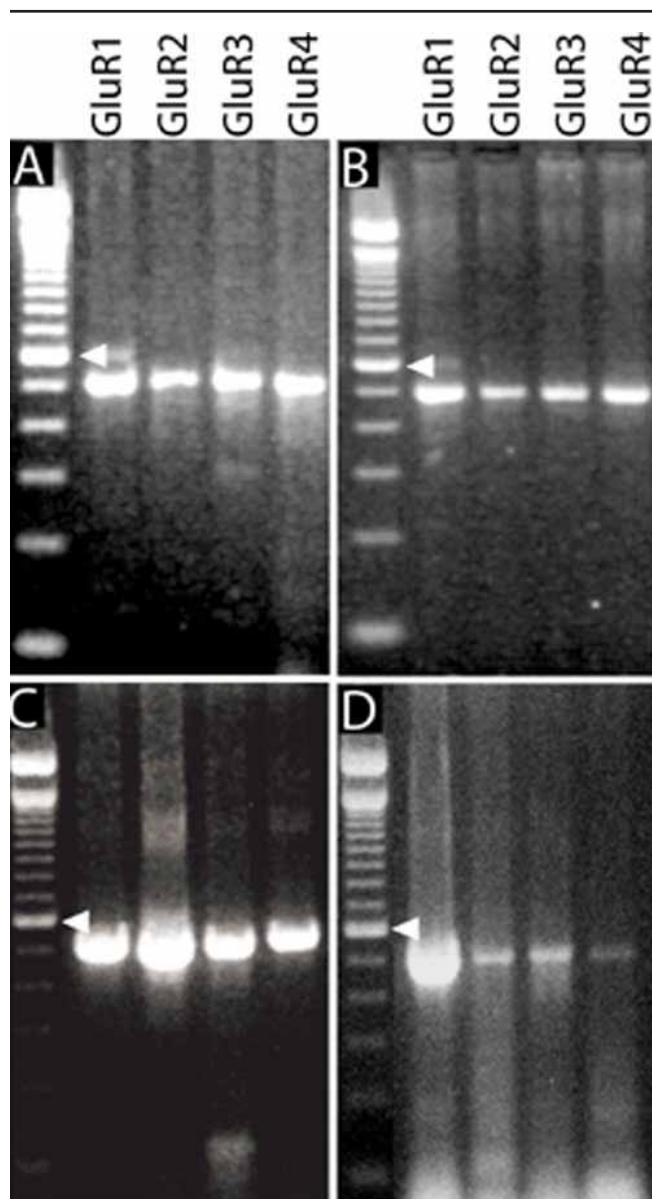


Figure 3. Comparison of AMPA receptor mRNA in retina and brain. **A,B:** Detection of mRNA for AMPA receptor subunits GluR1-4 in samples from two different macaque retina. **C:** Detection of same genes in sample of macaque brain (frontal lobe) following TPEA RT-PCR. **D:** Detection of AMPA receptors from cDNA library constructed from human brain RNA. No AMPA receptor mRNAs were detected when reverse transcriptase was omitted (data not shown). Initial amplification using TPEA-PCR was completed with the same primers for all tissues. All gene-specific PCR reactions were completed at 35 cycles. Arrowheads indicate 600 base pairs.

cific identity. The gene-specific PCR for the AMPA subunits confirms that the amplification of similar genes remains linear at approximately the same rate. Moreover, multiple genes can be detected from the same original RNA pool using subunit-specific primers, despite possible variations in gene structure and quantity.

We confirmed that expression of genes encoding AMPA receptors is similar for a second cDNA library from a different macaque retina using the same set of primers (compare Figure 3A,B). We also compared AMPA expression in the retina with expression in a cDNA library constructed from macaque frontal lobe (Figure 3C) and in a library constructed from human brain total RNA (Figure 3D). Expression of GluR1-4 is qualitatively similar between macaque retina and brain, though expression levels for all four subunits are gener-

ally higher in brain than in retina. Expression of GluR2-4 in human brain appears to be lower than in the macaque tissue (compare Figure 4C,D), with a greater abundance of GluR1. While comparisons are unable to be made between different gene products in a given tissue due to variations in primer efficiency, comparisons can be made between the same gene and different tissues [36]. Decreased strengths for the GluR2-4 reactions in human brain maybe due to lower levels of expression in the area of the brain in which the RNA was extracted, or because of a lessened proportion of mRNA to total RNA for these genes.

We then determined the general pattern of expression for genes encoding the kainate receptor subunits using TPEA PCR (Figure 4), having first established that the linear ranges for these genes are similar to those for the AMPA receptors (not shown). In the same two retina used for detection of the AMPA receptors (Figure 3A,B), we detected a high abundance of both GluR5 and GluR6, strong but lesser expression of KA2, and relatively little GluR7 and KA1 (Figure 4A,B). The patterns are highly similar for both retinas. We obtained similar results for the same two retinas using a different set of primers (not shown). Thus, the relatively low levels of mRNA encoding GluR7 and KA1 and the differences in expression between subunits that we detect do not appear to be due to our choice of primers as they amplify the gene products in human brain significantly. While expression in macaque brain for the kainate receptors is similar to that of the retina, there are subtle differences. Like the retina, expression of GluR5, GluR6, and KA2 are significantly higher than KA1 (Figure 4C). However, in the macaque brain, GluR7 is only slightly less abundant than GluR5. Finally, for human brain cDNA, GluR6, and KA2 are most highly expressed, with GluR5, GluR7, and KA1 only slightly less abundant (Figure 4D). Thus, while all kainate receptor subunits are expressed in these tissues, there are subtle differences in the relative expression of each.

We ascertained mGluR expression from the same cDNA libraries used for the GluR subunits. Each of mGluR1-8 was detected in both examples of macaque retina (Figure 5A,B). Not surprisingly, mGluR6 was the most highly abundant mGluR detected in the retina [37]. Since PCR products for mGluR2 were so low, multiple sets of mGluR2 primers pairs were used for gene-specific PCR and expression was confirmed (data not shown). These same primers were used to determine large portions of the mGluR2 coding region in macaque retina cDNA (Table 3), further confirming the expression. PCR products of equal size were also detected in macaque and human brain (Figure 5C,D) and include mGluR6. While mGluR6 has often been thought to be retina specific, we are not the first to detect mGluR6 in brain using RT-PCR [38]. The relative expression level for mGluR6 in the retina is greater than the other mGluRs, while in macaque brain the expression levels are similar, with the exception of mGluR5, for which expression is less. In human brain (Figure 5D), expression of mGluR7 and mGluR8 is higher than that of mGluR1-6. Additionally, when primers were used to amplify a region of mGluR8 spanning the stop codon, we found two distinct PCR products (data not shown, but represented in GenBank by accession num-

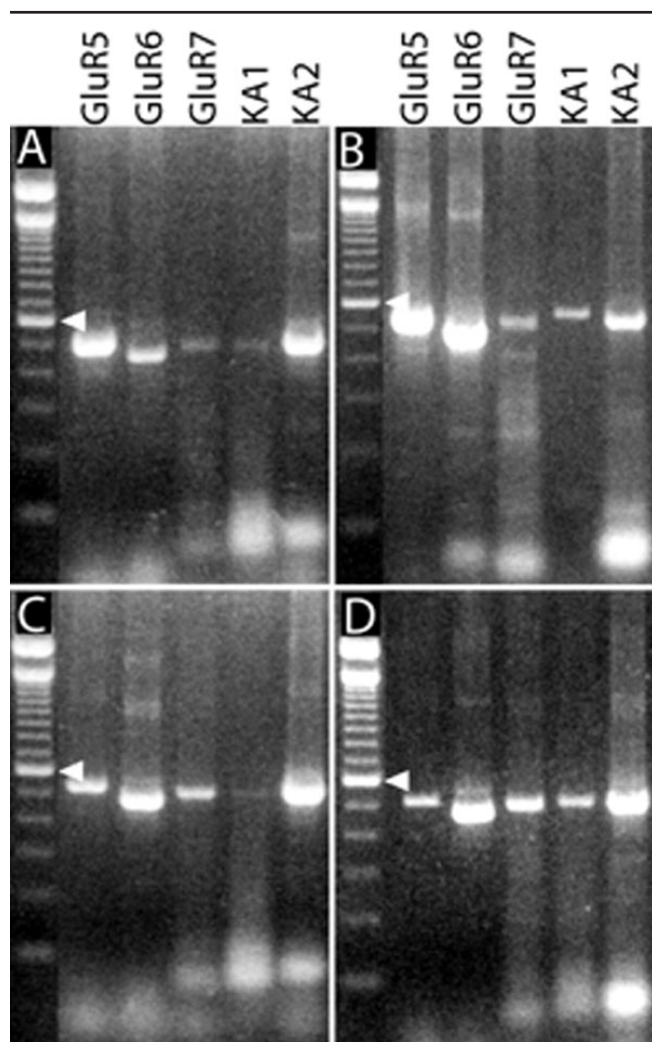


Figure 4. Expression of kainate receptor genes in retina and brain. **A,B:** Detection of mRNA encoding the kainate receptor subunits GluR5-7 and KA1-2 in samples from two different macaque retina. Similar results obtained for detection of the same genes in samples of macaque frontal lobe (**C**) and human brain RNA (**D**). No PCR products were detected when reverse transcriptase was omitted (data not shown). All PCR reactions as described for Figure 3. Arrowheads indicate 600 base pairs.

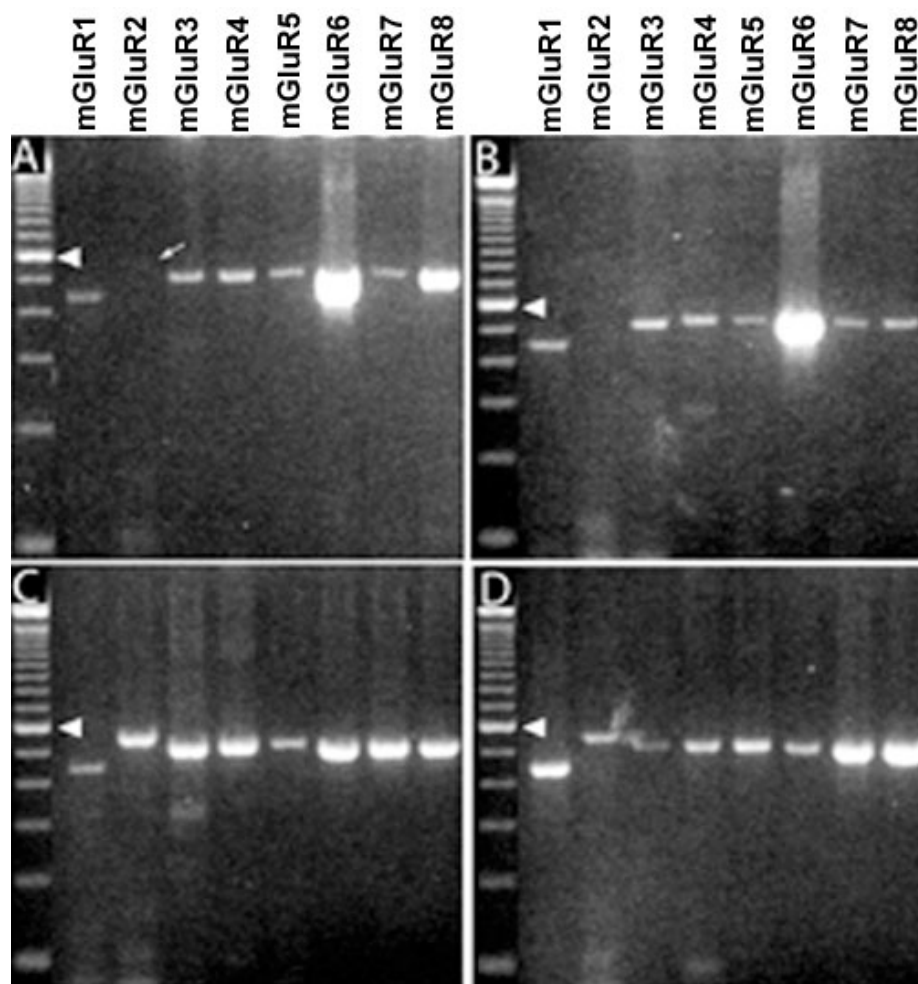


Figure 5. Determination of mGluR receptor gene expression in retina and brain. **A,B:** Detection of mRNAs encoding the metabotropic receptors mGluR1 through mGluR8 in samples from two different macaque retina. Similar results obtained for detection of same genes in samples of macaque frontal lobe (**C**) and human brain RNA (**D**). No PCR products were detected when reverse transcriptase was omitted (data not shown). All PCR reactions as described for Figure 3. Arrowheads indicate 600 base pairs.

TABLE 3. SUMMARY OF SEQUENCES OBTAINED FOR MACAQUE GLUTAMATE RECEPTORS

Gene	GenBank number	Nucleotides sequenced	% coding region sequenced	Coding homology	
				Nucleotide	Amino acid
GluR1	DQ159929	3237	100	98.2	99.8
GluR2	DQ159930	3206	100	97.5	98.8
GluR3	DQ159931	3009	100	98.1	99.4
GluR4	DQ159932	2709	100	97.9	98.0
GluR5	DQ159933	2863	100	98.3	99.9
GluR6	DQ159934	2729	100	99.0	99.7
GluR7	DQ159935	3634	100	98.0	99.8
KA1	DQ159936	2582	89.9	about 99.1	about 99.9
KA2	DQ159937	2700	90.9	97.9	about 99.7
mGluR1	DQ417741-DQ417743	3697	91.4	about 97.7	about 98.3
mGluR2	DQ417744-DQ417745	2145	81.9	about 98.0	about 99.5
mGluR3	DQ417734	2988	100	98.3	99.4
mGluR4	DQ417735	3495	100	97.5	99.7
mGluR5	DQ417746-DQ417747	2205	60.0	about 98.5	about 93.2
mGluR6	DQ417748	2071	78.7	about 95.9	about 97.7
mGluR7	DQ417749	2746	87.8	about 98.4	about 99.8
mGluR8a	DQ417750	1865	57.8	about 98.7	about 99.2
mGluR8b	DQ417751	1920	57.8	about 98.7	about 99.2

“Accession number” represents GenBank accession number for new macaque sequence. “Nucleotides sequenced” represents total number of nucleotides sequenced, including and beyond coding region. “% coding region sequenced” represents fraction of coding region included in the total number of nucleotides sequenced. “Coding homology, Nucleotide” represents nucleotide homology and refers to nucleotides sequenced within coding region, while “Coding homology, amino acid” refers to translation predicted from the coding sequence.

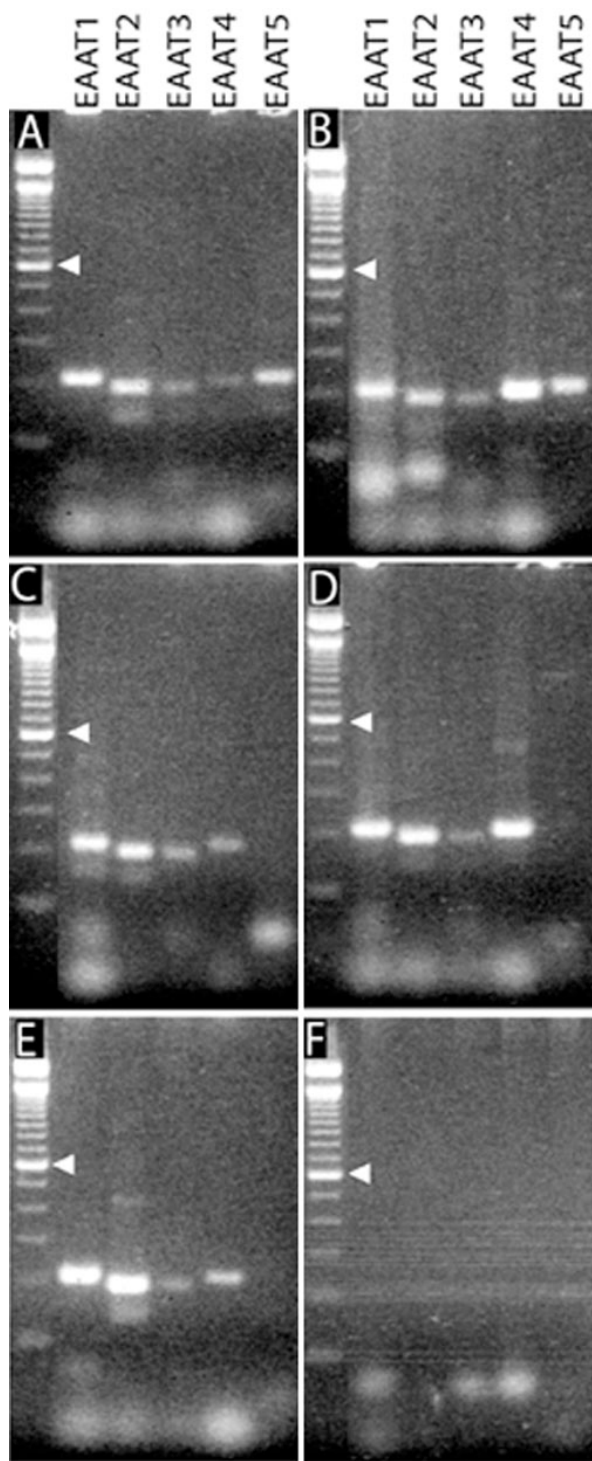


Figure 6. Expression of mRNA for non-vesicular glutamate transporters in retina and brain. **A,B**: Detection of specific genes encoding glutamate transporters EAAT1 through EAAT5 in samples from two different monkey retina following construction of cDNA library using TPEA RT-PCR. Detection of same genes in sample of monkey brain (frontal lobe; **C**), monkey cerebellum (**D**) and total human brain cDNA libraries (**E**). **F**: No glutamate transporter mRNA in monkey retina were detected when reverse transcriptase was omitted. All PCR reactions as described for Figure 3. Arrowheads indicate 600 base pairs. Primers for gene-specific PCR and expected sizes are listed in Table 1. **A-E**: mRNA encoding EAAT5 is present in primate retinal tissue only while EAAT4 is present in retina and cerebellum.

bers DQ417750 and DQ417751; Table 3). Subsequent sequencing of these PCR products revealed the known isoforms mGluR8 (or mGluR8a; NM_000845), and mGluR8b (AJ236921). The mGluR8b product includes the out-of-frame insertion of 55 base pairs at nucleotide 2734 of the mGluR8 isoform. This insertion contains a new stop codon, and replaces the last 16 amino acid residues in the C-terminus of mGluR8 with 16 different amino acid residues in mGluR8b.

Next we compared the expression of the non-vesicular glutamate transporters EAAT1-5 in the same tissue sets. In addition, we probed for these transporters in cerebellum, as EAAT4 is predominantly associated with glutamate transport by cerebellar Purkinje cells [39,40]. Gene-specific PCR demonstrates expression of all five transporters in the two examples of macaque retina (Figure 6A,B). These results correspond to the recent discovery of EAAT4 expression in human and other mammalian retinas [41,42]. In addition, we find EAAT5 expression in the retina only (Figure 6A-E). This concurs with the previous finding of much lower expression of EAAT5 in brain [43].

Macaca versus human sequences: Our results indicate substantial differences in the expression levels of specific glutamate receptors and transporters between macaque retina and brain and between the macaque and human cDNAs. We began each gene-specific PCR reaction with an equivalent amount of cDNA, and all the primer pairs we used were optimized for the human sequences with regard to annealing temperature and amplification rates. Thus, we wondered whether the variation in PCR product intensities could arise not from differences in the actual expression levels, but from differences between the macaque and human sequences. To resolve this issue, we attempted to determine for the macaque retina the full-length sequence for each glutamate receptor whose expression levels we studied for comparison with the human homologues found in GenBank (accession numbers in Table 1). Only small fragment sequences of the non-vesicular glutamate transporters were determined to confirm PCR product specificity and are available at Genbank (accession numbers DQ417736, DQ417737, DQ417738, DQ417739, DQ417740).

We produced contiguous sequence information using an iterative process of fragment sequencing and aligning for each of the AMPA and kainate subunits as well as mGluR receptors whose expression pattern we studied. We designed primer pairs to amplify the corresponding gene fragment based on the human sequence, and when positive, the PCR product from monkey retina was purified and sequenced. Whenever possible, we continued our nucleotide sequencing on both sides of the coding region. Figure 7 illustrates our procedure for the AMPA subunit GluR1. Three positive PCR reactions for distinct GluR1 fragments of approximately 500 base pairs each are separated by empty lanes (Figure 7A), before precipitation and electrophoreses, alongside a DNA mass ladder to determine sample concentrations (Figure 7B). The majority of bands were slightly below the intensity of the 800 base pair band in the ladder. The relative intensities equate to just less than 20 ng/ μ l in these samples. Quantifying samples in this manner,

rather than with a spectrophotometer, allowed us to confirm the purity of our samples as well. Figure 7C represents the finished assembly of the GluR1 gene from the component PCR products. Like all of the GluR subunits we sequenced, the coding region for GluR1 is approximately 2700 base pairs in length.

We sequenced between 1865 (mGluR8a) and 3697 (mGluR1) total nucleotides for each gene and were able to complete coding sequences for GluR1-7, mGluR3 and mGluR4 (Table 3). We also obtained nearly complete sequences for KA1-2, mGluR1-2, and mGluR5-8. We made nucleotide comparisons between the available monkey sequence from retina and the analogous human sequence. We calculated nucleotide homology for partial genes by comparing only the completed, continuous portion of the macaque sequence with the corresponding portion of the human sequence. The corresponding homologies to the human sequence are listed in Table 3. The nucleotide coding sequences contain as many as 68 differences (mGluR4) or as few as 26 (GluR6). Table 3 lists homologies

and accession numbers for each submitted contiguous sequence.

We translated the coding region on the direct strand of each gene to a predicted amino acid sequence. We calculated amino acid identity for genes in which the start codon was known and the protein sequence remained in-frame, as well as incomplete genes when the reading frame could be inferred. Many of the differences in the nucleotide coding sequence occur at the wobble or third codon position and therefore lead to the same amino acid. Thus, the homologies in amino acid sequence between *macaca* and human are always higher than the nucleotide homologies (Table 3). The differences in nucleotide sequence lead to as many as 18 changes in the amino acid sequence of the coded protein (GluR4) or as few as one (GluR5).

Detection of glutamate receptors and transporters in fixed tissue: Our objective in the companion paper is to determine glutamate receptor and transporter expression in single neurons pre-labeled using cell-specific markers in paraformaldehyde

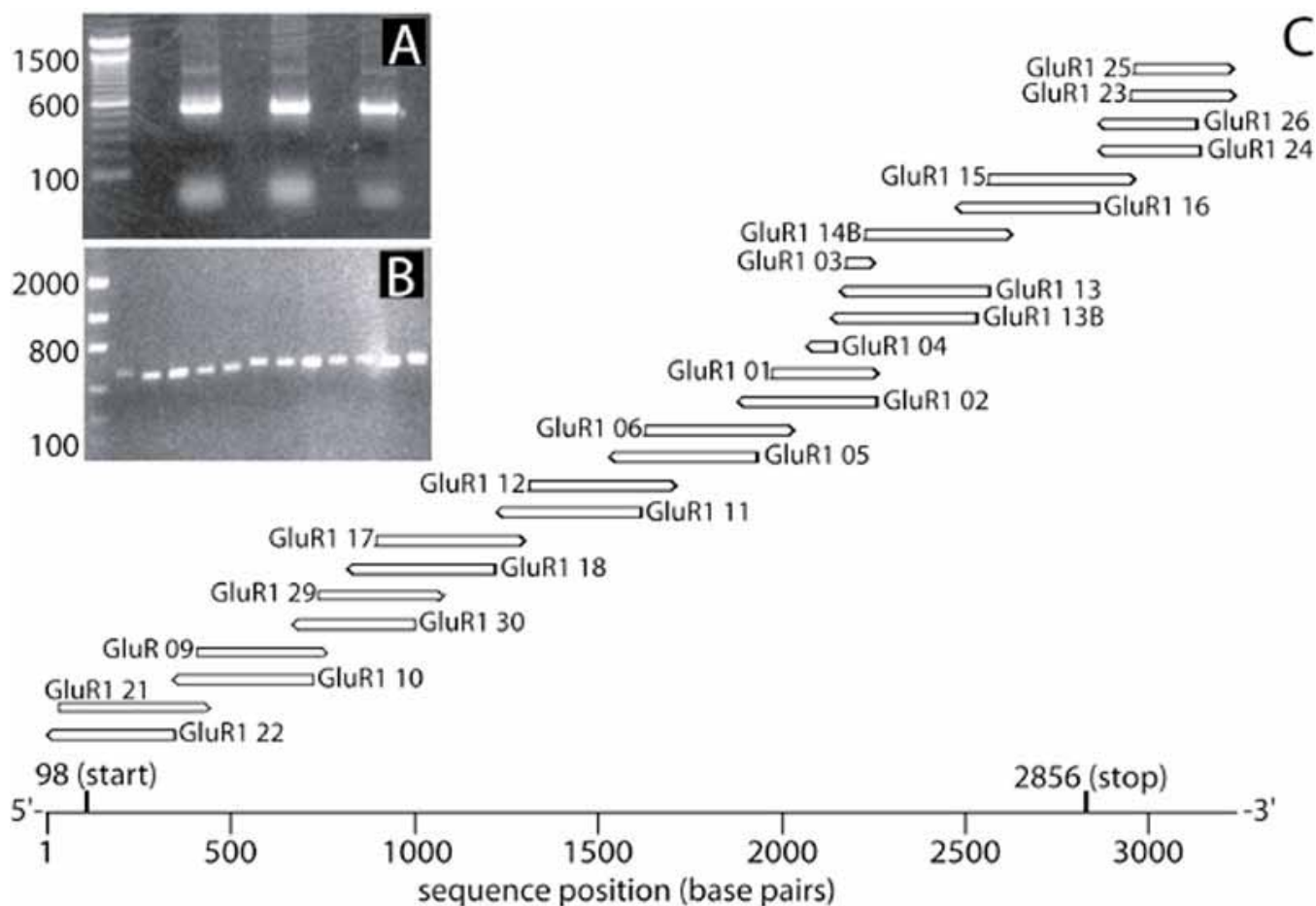


Figure 7. PCR fragment purification and sequencing for macaque retina illustrated for GluR1. **A:** Electrophoresis separation of three PCR products generated with independent primer sets against overlapping fragments of GluR1; samples were separated by empty lanes to prevent spillover. **B:** Comparison of a single GluR1 PCR product against a low DNA mass ladder for determining quantity of product for sequencing. **C:** Assembly of GluR1 fragments to generate the full-length coding region from a total of 3237 sequenced nucleotides. Primers were designed to produce an overlap of at least 100 base pairs for each PCR product.

fixed retinal slices. Here we set out to determine if enough RNA could be extracted from a fixed slice to create cDNA libraries using the TPEA RT-PCR method. In addition, we compared the expression of glutamate receptors and transporters in fixed mRNA to that in fresh tissue. Table 2 lists unique primers designed to generate products that ranged from 180-220 base pairs for each gene. Figure 8 compares gene-specific PCR to detect kainate receptors in cDNA libraries created from RNA extracted from fresh retina (Figure 8A) and a fixed (Figure 8B) retinal slice. While the overall expression of each gene appeared slightly greater in the fresh tissue, the relative expression of the genes remained the same. Sequencing PCR products from the fixed tissue confirmed primer specificity and ruled out false positives, as with the PCR products from fresh tissue.

While care in primer design is necessary for fixed tissue, we used TPEA to detect mRNAs encoding GluR1-7, KA1-2, mGluR1-8, and EAAT1-5 (Figure 8B-E). We confirmed the

absence of PCR products in RNA extracted from fixed tissue with reverse transcriptase omitted during the initial first strand synthesis or with primers designed to genomic DNA (data not shown). As a positive control, we performed gene-specific PCR on a fresh retina cDNA library using the same set of primers to ensure comparable generation of PCR products for all receptors and transporters (data not shown). Gene-specific PCR amplification at a relatively low PCR cycle number, 35, and at a moderately high annealing temperature, 60 °C, reduced false positives and nonspecific signals. We performed gene-specific PCR reactions twice to ensure consistent results.

DISCUSSION

Using TPEA to generate whole-retina cDNA: Our objective was to determine whether TPEA RT-PCR is suitable for amplification of low-abundance transcripts and for transcripts of various lengths expressed in primate retina. We constructed full-complement cDNA libraries from two macaque retina

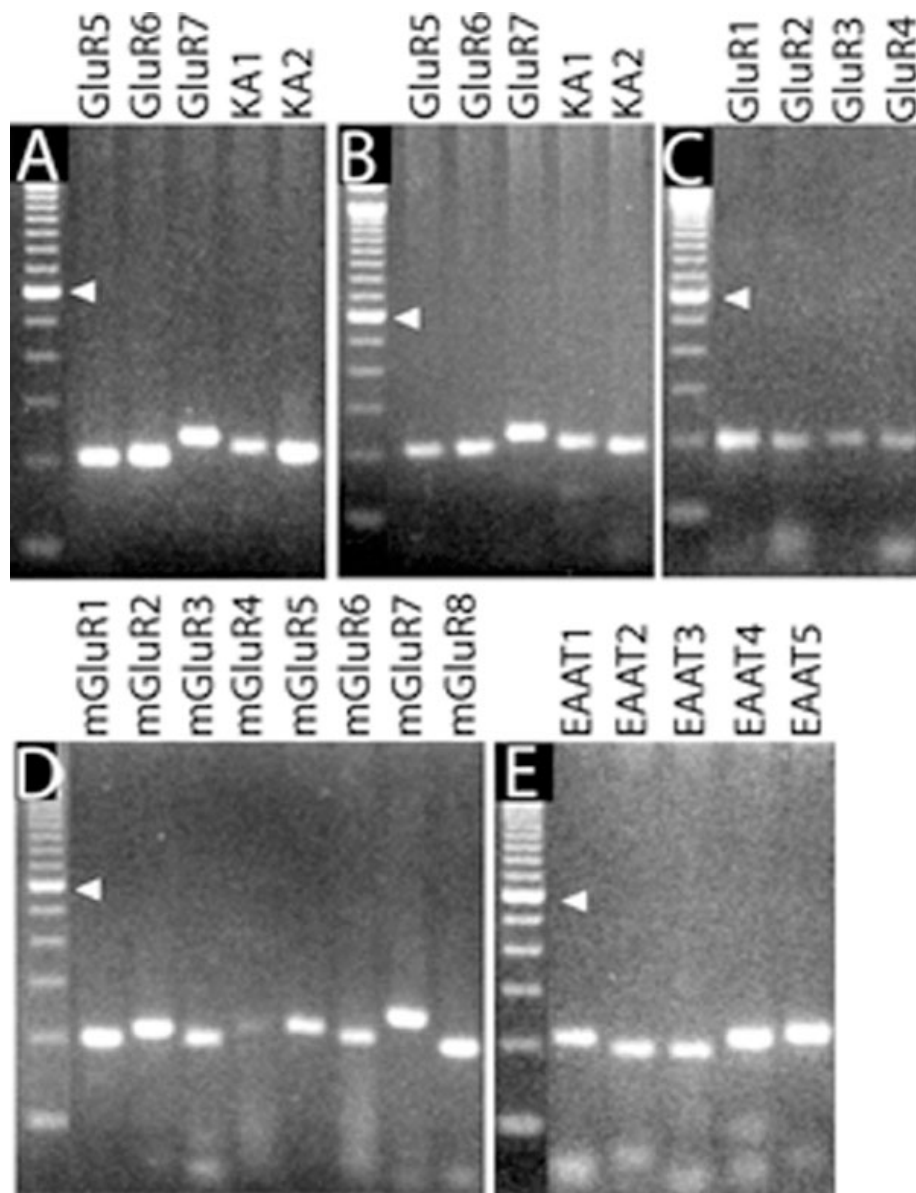


Figure 8. Glutamate receptor and transporter detection in primate retina from fixed tissue. **A,B:** Detection of specific genes encoding the kainate receptor subunits GluR5-7 and KA1-KA2 in samples from fresh and fixed monkey retina following construction of cDNA libraries using TPEA RT-PCR. Gene-Specific PCR demonstrates that kainate receptors can be identified from fresh (**A**) or fixed tissue (**B**). **C-E:** Each of the AMPA, mGluR and EAAT genes can also be detected in fixed tissue. No genes were detected when reverse transcriptase was omitted (data not shown). Arrowhead indicates 600 base pairs. Primers used for gene-specific PCR and expected product sizes are the same as for Figure 6 and listed in Table 1.

using TPEA, probed these libraries for glutamate receptor and transporter expression, continued by comparing their coding sequences to their human orthologs, and demonstrate gene-specific feasibility in RNA extracted from fixed tissue. Originally, second strand synthesis in TPEA uses a primer that contains a stretch of five random nucleotides and a defined pentameric sequence [1]. Assuming a completely random length of nucleotide sequence, we would expect that a given sequence of five base pairs would appear every 1024 base pairs (4^5), even though some nucleotide sequences are more common than others. Our modification of this protocol contained a combination of four such primers, so we anticipated that a greater length of gene from the 3' end would be selected and amplified, even in the presence of a large 3' untranslated region. Our results in Figure 1 bore this out, showing amplification and detection of significantly large transcripts, even those a considerable distance from the poly-A tail. For mGluR6 (Figure 1A), the length of the untranslated region from the

poly-A tail to the stop codon is 3309 base pairs, and furthermore, we amplified and sequenced nucleotides in the mGluR1 subunit as far as 6311 bases from the poly-A tail. We also tried to limit any potential 3' bias by placing our initial amplification of specific genes 1000 bases into the coding sequence.

The TPEA method amplifies high and low abundant genes equally, because amplification primers do not anneal to any particular gene or region. However, a forgotten and often ignored parameter in comparing gene expression via PCR is the size of the products generated. Based on our experience, for a given reaction cycle and constant quantity of cDNA, small amplicons reach maximum amplification quicker than larger amplicons. In order to account for differences in amplification rates of different sized products, we designed all our gene-specific primers to produce approximately 500 base pair products. Thus, by keeping these parameters equivalent, we were able to compare different genes within a particular sample of tissue.

TABLE 4. PREDICTED AMINO ACID CHANGES FOR MACAQUE SEQUENCES COMPARED TO HUMAN

Gene	Coding substitutions	Amino acid positional changes (position: human to macaca)
GluR1	48 (2758)	375: S to G, 870: A to G
GluR2	67 (2652)	14: V to I, 241: E to G, 765: T to N, 766: P to A, 779: V to L, 796: A to S 797: K to G, 798: D to G, 799: S to G, 800: G to D
GluR3	51 (2682)	10: S to N, 563: Y to S, 807: S to T, 810: G to C, 811: D to G
GluR4	58 (2709)	54: S to A, 273: I to T, 327: N to K, 328: A to S, 732: E to D, 733: Y to N 767: A to P, 776: N to S, 778: P to A, 780: L to V 765: G to R, 766: N to T, 797: S to P, 798: G to K, 799: G to D, 800: G to S, 801: D to G, 884: A to T
GluR5	47 (2755)	3: H to L
GluR6	26 (2724)	567: I to V, 571: Y to C, 621: Q to R
GluR7	54 (2760)	199: I to V, 310: S to A
KA1	greater than or equal to 22 (2582)	391: H to R
KA2	greater than or equal to 57 (2700)	298: L to P, 809: I to V
mGluR3	45 (2646)	46: N to K, 534: P to S, 549: S to P, 593: V to I, 858: T to M
mGluR4	68 (2739)	5: S to R, 66: A to P, 584: D to G

"Coding substitutions" represents number of substituted nucleotides in coding region with total number of coding nucleotides sequenced contained in parentheses. "Amino acid positional changes" represents the position in translated protein and the change in amino acid from human to macaque retina, using standard abbreviations.

Expression of AMPA and kainate subunits in retina: Both in situ hybridization studies and RT-PCR have shown a widespread and differential distribution of GluR subunit mRNAs throughout the mammalian retina [8,22-25]. By probing whole retina cDNA, we have demonstrated the relative expression of the four AMPA-sensitive subunits (GluR1-4; Figure 3) and the five kainate-sensitive subunits (GluR5-7, KA1-2; Figure 4), including the first demonstration of GluR3, GluR6, GluR7 as well as KA1 expression in the primate retina. Nonspecific antibodies to GluR2/3 and GluR6/7 [14,15,44,45] suggest subunit expression and their expression is definitively shown here. RT-PCR from human retinoblastoma cell lines also suggests KA1 gene expression with our results confirming this in primary tissue [18]. Gene-specific PCR for each AMPA subunit over a wide range of PCR cycles not only validated the linearity of our method of cDNA construction and the specificity of subunit detection, but also demonstrated that expression levels between the subunits are approximately equal (Figure 2).

Gene-specific PCR for the kainate receptor subunits demonstrates that the low-affinity subunits GluR5 and GluR6 and the higher affinity KA2 subunit are consistently and highly expressed across two different macaque retinas, while GluR7 is expressed to a lesser degree, and KA1 is expressed very little, if at all (Figure 4). While additional data from primate retina are not available, in situ hybridization and other studies of mammalian retina support these results [46]. In both cat and rat retina, mRNA encoding GluR5 and GluR6 are both more heavily expressed than the mRNA for GluR7 [22,47,48]. In rat retina, the gene for KA2 is far more heavily expressed than the gene for KA1, which may be absent [49]. Our PCR also suggests that both GluR5 and GluR6 are more prevalent than the KA2 subunit (Figure 4).

Certain immunocytochemical studies also support our results for the relative expression of the particular subunits. Brandstätter et al. [9] found in rat retina more pronounced localization of GluR6/7 than the KA2 subunit. For the macaque retina, Haverkamp et al. [14] demonstrated a highly focal localization of KA2 to the outer retina, with more widespread localization of GluR5 and GluR6/7; GluR6/7 was also more highly expressed than GluR5. Using subunit-specific antibodies, Qin and Pourcho [13] demonstrated in cat retina that GluR7 is again most weakly expressed, with more prominent expression of both GluR5 and GluR6. While not quantitative, the immunocytochemical data as a whole support the PCR results demonstrating higher levels of GluR5 and GluR6 than of GluR7, KA1, or KA2.

High levels of GluR7 detection in monkey and human brain suggest that the low abundance in retina is not due to primer inefficiency and to the use of primers designed against the human sequence (Figure 4). In fact, over 30 PCR reactions using different sets of primers designed to regions spanning the entire GluR7 gene revealed consistently lower expression in the monkey retina compared to monkey brain (data not shown). For these reactions, GluR7 was often undetectable in retina while easily detected in monkey and human brain. Similarly, Hinoi & Yoneda [25], investigating kainate receptor expression in rat adenohypophis, were unable to detect

GluR7 mRNA in rat retina, despite detection of the other kainate subunits.

Expression of metabotropic glutamate receptors in retina: Despite the critical importance of mGluRs in visual processing [50-52], only mGluR6 has been localized in primate retina [53,54]. Hartveit et al. [55] showed mGluR1-2 and mGluR4-7 gene expression in the rat retina via in situ hybridization and supported their own results with immuno-localization [56]. Subsequently, mGluR subunits have been localized in various non-primate mammalian retina [55,57]. Here we demonstrated expression of all genes encoding mGluRs (mGluR1-8) in the primate retina (Figure 5). Although the initial amplification of mGluR2 was lower in retina than brain tissue, and was in fact barely detectable, we are confident of its expression in retina, as multiple primer pairs were used to amplify products while attempting to determine full-length sequences of retina mGluR2.

While attempting to determine the full-length sequence for mGluR8, we verified the expression of two isoforms of the receptor, mGluR8(a) and mGluR8b, as demonstrated in other mammals [58]. The mGluR8b isoform is identical to that of mGluR8 except for an out-of-frame insertion of 55 base pairs at nucleotide 2734 of the mGluR8 isoform. The insertion contains a stop codon, and replaces the last 16 amino acid residues in the C-terminus of mGluR8 with 16 different amino acid residues in mGluR8b. In previous studies, the protein for the mGluR8b isoform was never detected in retina because the antibody used was raised against the last 19 amino acids whose continuous sequence in mGluR8 is interrupted in mGluR8b by the insertion [59,60]. We detected both splice variants mGluR8a and mGluR8b in monkey retina, cortex, cerebellum, and human total brain (data not shown). Malherbe et al. [61] also describes an mGluR8c isoform that contains a different 74 base pair out-of-frame insertion at nucleotide 1413. We could not detect this isoform in our retina cDNA library.

The expression of mGluR6 appeared highest among the mGluRs in the retina (Figure 5). These results are not surprising since mGluR6 has long been thought to be highly expressed in the retina and in fact to be retina specific [37]. However, we detected mGluR6 in brain, as have others [38]. In that study, as with ours, two rounds of PCR were used to detect mGluR6, thus enabling detection of even low levels of the gene. An alternative is that mGluR6 mRNA is transcribed in non-retinal tissue, but not translated into protein, although this result is highly unlikely.

Expression of glutamate transporters in retina: Numerous studies of the expression and localization of EAAT subunits in the retina have suggested the absence of EAAT4 and exclusive expression of EAAT5 [62]. Recent evidence demonstrates EAAT4 mRNA and protein in retina of rat [42] and human [41]. Generation of gene-specific EAAT4 PCR products from our retinal cDNA libraries supports these results in macaque. EAAT4 is known to be expressed within a number of regions of the central nervous system, but is predominantly associated with glutamate transport by Purkinje cells within the cerebellum [40,63,64]. Expression of EAAT4 has been shown to be much higher in cerebellum compared to frontal

cortex and retina [42]. Our results support this with consistently higher expression within cerebellum, although expression in one retina was substantial (Figure 6).

The EAAT5 transporter appears to be a retina-specific transporter whose presence in photoreceptor cells provides for rapid uptake of glutamate at the first retinal synapse [43]. In the primate retina staining for EAAT5 was confined to rod terminals [62]. Our gene-specific PCR also suggests retina specific expression. During multiple attempts at amplifying EAAT5, we could not detect a product in macaque cortex, cerebellum or human brain (Figure 6). Thus our results support the concept that the retina expresses all five EAATs, while other brain tissues appear to express only four.

Comparison of macaque and human sequences: With respect to understanding human gene function, the use of experimentally amenable model organisms has been an important paradigm in basic biomedical research. Comparative DNA sequence studies between humans and non-human primates are critical for understanding the genetic basis for phenotypic differences between the species. We compared large portions of genes encoding glutamate receptors and transporters in monkey retina with their human orthologs available in GenBank. The iterative process of full-length gene construction was employed to try to eliminate spontaneous errors caused by misreading during PCR. By using multiple PCR reactions and products, overlapping by at least 100 base-pairs at both 5' and 3' ends, we were able to confirm correct sequence calls that may be missed by amplification of the entire gene in only a single reaction. In addition, most parts of full-length genes were determined with quadruple coverage.

Following complete sequencing of the coding regions for several glutamate receptors, amino acid structures were predicted and compared to human. The predicted amino acid changes and their relative positions in each completed gene are listed in Table 4. Most nucleotide differences did not result in an amino acid change, since they occurred at the wobble or third position. For example, for GluR5, 47 nucleotide substitutions in the macaque sequence lead to only a single amino acid change: histidine is replaced by a leucine at position three in the amino acid coding sequence. The three kainate receptors for which we were able to determine full length sequences (GluR5-7) seem more evolutionarily conserved between monkey and human than the AMPA receptors. In these, large insertions exist in both monkey and human at the 5' end, when compared to the mouse sequence. However, GluR5 does contain two amino acids at 567 and 621 that are equivalent in monkey and mouse, but not in human.

While the percent homology between mGluR3 may seem unusually low (98.3%) for such a highly conserved gene between closely related species, we are confident of the nucleotide differences between the macaque and human transcripts. In fact, of the 49 nucleotide changes we determined between macaque and human mGluR3, 35 have been confirmed by an independent group that cloned mGluR3 from macaque brain (GenBank accession number AB169807).

Unfortunately, not all full-length genes were decipherable. For example we could not amplify all of KA1 and KA2

either in macaque retina or in macaque brain. However the gaps are not due to improper library construction, as the missing nucleotides in KA1 and KA2 occur at the 3' end of the sequence, including the stop codon. That GluR7 and KA1 expression is relatively low in the monkey retina probably contributed to decreased amplification of the genes at the missing portions. However, this cannot be the sole reason for our inability to complete the sequences, which we believe is most likely due to actual differences between the macaque and human sequences. In dozens of instances, we amplified regions of KA1 and KA2 in human brain and not in monkey retina or brain. If primers differ from the gene sequence by as little as one nucleotide at the 3' end of the primer, amplification will be compromised.

Gene detection in fixed tissue: TPEA was originally described for use with single cells [1]. As a first step toward using TPEA to study gene expression in single cells from paraformaldehyde-fixed, immuno-labeled retinal slices, we used TPEA for gene-specific PCR of RNA extracted from a single, fixed slice (Figure 8). As demonstrated by Specht et al. [33] through a thorough examination of multiple methodologies, digestion with Proteinase K (Ambion Inc., Austin, TX) at high temperature followed by organic extraction yields high levels of RNA and highly reproducible results, as compared to other RNA extraction methodologies. This study demonstrated that the protease was capable of efficiently degrading proteins that were covalently cross-linked to the RNA, thereby allowing more efficient extraction than chaotropic agents. The study also found that amplicon sizes up to approximately 200 bp gave the best results for gene detection. Amplification protocols that involved only small RNA target sequences proved to be most successful, presumably because of the significantly reduced risk of cross-link occurrence in the region bordered by the PCR primers. Therefore all our primers were designed to yield PCR products between 180-200 bp. When larger amplicons were tested (>250 bp), detection of these products were sporadic at best (data not shown).

Our direct comparison using the same digestion technique and short primers with fresh macaque retina demonstrated a comparable range of detection of the kainate receptors (Figure 8). This indicates that similar results can be obtained using TPEA for either fresh or fixed RNA. Also, as with fresh RNA, we could extract enough RNA from the fixed slice to probe for well over 20 different genes. Doing so, we found similar expression in the fixed slice of all AMPA, kainate and mGluRs, as well as the five non-vesicular glutamate transporters. These results set the stage for studying expression in single retinal cells extracted from fixed tissue [32].

ACKNOWLEDGEMENTS

Funded by NIH grant EY12480, the Sloan Foundation and a Wasserman Award to DJC from Research to Prevent Blindness, Inc.

REFERENCES

1. Dixon AK, Richardson PJ, Lee K, Carter NP, Freeman TC. Expression profiling of single cells using 3 prime end amplifica-

- tion (TPEA) PCR. *Nucleic Acids Res* 1998; 26:4426-31.
2. Thoreson WB, Witkovsky P. Glutamate receptors and circuits in the vertebrate retina. *Prog Retin Eye Res* 1999; 18:765-810.
 3. Kalloniatis M, Tomisich G. Amino acid neurochemistry of the vertebrate retina. *Prog Retin Eye Res* 1999; 18:811-66.
 4. Dingledine R, Borges K, Bowie D, Traynelis SF. The glutamate receptor ion channels. *Pharmacol Rev* 1999; 51:7-61.
 5. Conn PJ, Pin JP. Pharmacology and functions of metabotropic glutamate receptors. *Annu Rev Pharmacol Toxicol* 1997; 37:205-37.
 6. Pin JP, Duvoisin R. The metabotropic glutamate receptors: structure and functions. *Neuropharmacology* 1995; 34:1-26.
 7. Kristensen BW, Noraberg J, Zimmer J. Comparison of excitotoxic profiles of ATPA, AMPA, KA and NMDA in organotypic hippocampal slice cultures. *Brain Res* 2001; 917:21-44.
 8. Peng YW, Blackstone CD, Haganir RL, Yau KW. Distribution of glutamate receptor subtypes in the vertebrate retina. *Neuroscience* 1995; 66:483-97.
 9. Brandstatter JH, Koulen P, Wassle H. Selective synaptic distribution of kainate receptor subunits in the two plexiform layers of the rat retina. *J Neurosci* 1997; 17:9298-307.
 10. Morigiwa K, Vardi N. Differential expression of ionotropic glutamate receptor subunits in the outer retina. *J Comp Neurol* 1999; 405:173-84.
 11. Qin P, Pourcho RG. AMPA-selective glutamate receptor subunits GluR2 and GluR4 in the cat retina: an immunocytochemical study. *Vis Neurosci* 1999; 16:1105-14. Erratum in: *Vis Neurosci* 2000; 17:155.
 12. Qin P, Pourcho RG. Localization of AMPA-selective glutamate receptor subunits in the cat retina: a light- and electron-microscopic study. *Vis Neurosci* 1999; 16:169-77.
 13. Qin P, Pourcho RG. Immunocytochemical localization of kainate-selective glutamate receptor subunits GluR5, GluR6, and GluR7 in the cat retina. *Brain Res* 2001; 890:211-21.
 14. Haverkamp S, Grunert U, Wassle H. Localization of kainate receptors at the cone pedicles of the primate retina. *J Comp Neurol* 2001; 436:471-86.
 15. Haverkamp S, Grunert U, Wassle H. The synaptic architecture of AMPA receptors at the cone pedicle of the primate retina. *J Neurosci* 2001; 21:2488-500.
 16. Grunert U, Lin B, Martin PR. Glutamate receptors at bipolar synapses in the inner plexiform layer of primate retina: light microscopic analysis. *J Comp Neurol* 2003; 466:136-47.
 17. Grunert U, Haverkamp S, Fletcher EL, Wassle H. Synaptic distribution of ionotropic glutamate receptors in the inner plexiform layer of the primate retina. *J Comp Neurol* 2002; 447:138-51.
 18. Naskar R, Vorwerk CK, Dreyer EB. Concurrent downregulation of a glutamate transporter and receptor in glaucoma. *Invest Ophthalmol Vis Sci* 2000; 41:1940-4.
 19. Eliasof S, Arriza JL, Leighton BH, Amara SG, Kavanaugh MP. Localization and function of five glutamate transporters cloned from the salamander retina. *Vision Res* 1998; 38:1443-54.
 20. Schultz K, Stell WK. Immunocytochemical localization of the high-affinity glutamate transporter, EAAC1, in the retina of representative vertebrate species. *Neurosci Lett* 1996; 211:191-4.
 21. Ward MM, Jobling AI, Puthussery T, Foster LE, Fletcher EL. Localization and expression of the glutamate transporter, excitatory amino acid transporter 4, within astrocytes of the rat retina. *Cell Tissue Res* 2004; 315:305-10.
 22. Hamassaki-Britto DE, Hermans-Borgmeyer I, Heinemann S, Hughes TE. Expression of glutamate receptor genes in the mammalian retina: the localization of GluR1 through GluR7 mRNAs. *J Neurosci* 1993; 13:1888-98.
 23. Hartveit E, Brandstatter JH, Enz R, Wassle H. Expression of the mRNA of seven metabotropic glutamate receptors (mGluR1 to 7) in the rat retina. An in situ hybridization study on tissue sections and isolated cells. *Eur J Neurosci* 1995; 7:1472-83.
 24. Zhang C, Hamassaki-Britto DE, Britto LR, Duvoisin RM. Expression of glutamate receptor subunit genes during development of the mouse retina. *Neuroreport* 1996; 8:335-40.
 25. Hinoi E, Yoneda Y. Expression of GluR6/7 subunits of kainate receptors in rat adenohypophysis. *Neurochem Int* 2001; 38:539-47.
 26. Ward MM, Jobling AI, Kalloniatis M, Fletcher EL. Glutamate uptake in retinal glial cells during diabetes. *Diabetologia* 2005; 48:351-60.
 27. Mimura Y, Mogi K, Kawano M, Fukui Y, Takeda J, Nogami H, Hisano S. Differential expression of two distinct vesicular glutamate transporters in the rat retina. *Neuroreport* 2002; 13:1925-8.
 28. Blackshaw S, Kuo WP, Park PJ, Tsujikawa M, Gunnerson JM, Scott HS, Boon WM, Tan SS, Cepko CL. MicroSAGE is highly representative and reproducible but reveals major differences in gene expression among samples obtained from similar tissues. *Genome Biol* 2003; 4:R17.
 29. Rauen T, Wiessner M. Fine tuning of glutamate uptake and degradation in glial cells: common transcriptional regulation of GLAST1 and GS. *Neurochem Int* 2000; 37:179-89.
 30. Mawrin C, Pap T, Pallas M, Dietzmann K, Behrens-Baumann W, Vorwerk CK. Changes of retinal glutamate transporter GLT-1 mRNA levels following optic nerve damage. *Mol Vis* 2003; 9:10-3.
 31. Rauen T, Taylor WR, Kuhlbrodt K, Wiessner M. High-affinity glutamate transporters in the rat retina: a major role of the glial glutamate transporter GLAST-1 in transmitter clearance. *Cell Tissue Res* 1998; 291:19-31.
 32. Calkins DJ, Hanna MC. Genomics of identified neuronal cell types in primate retina. ISER XV International Congress of Eye Research; 2002 October 6-10; Geneva, Switzerland.
 33. Specht K, Richter T, Muller U, Walch A, Werner M, Hofler H. Quantitative gene expression analysis in microdissected archival formalin-fixed and paraffin-embedded tumor tissue. *Am J Pathol* 2001; 158:419-29.
 34. Vardi N, Morigiwa K. ON cone bipolar cells in rat express the metabotropic receptor mGluR6. *Vis Neurosci* 1997; 14:789-94.
 35. Vardi N, Duvoisin R, Wu G, Sterling P. Localization of mGluR6 to dendrites of ON bipolar cells in primate retina. *J Comp Neurol* 2000; 423:402-12.
 36. Dyka FM, May CA, Enz R. Metabotropic glutamate receptors are differentially regulated under elevated intraocular pressure. *J Neurochem* 2004; 90:190-202.
 37. Nakajima Y, Iwakabe H, Akazawa C, Nawa H, Shigemoto R, Mizuno N, Nakanishi S. Molecular characterization of a novel retinal metabotropic glutamate receptor mGluR6 with a high agonist selectivity for L-2-amino-4-phosphonobutyrate. *J Biol Chem* 1993; 268:11868-73.
 38. Ghosh PK, Baskaran N, van den Pol AN. Developmentally regulated gene expression of all eight metabotropic glutamate receptors in hypothalamic suprachiasmatic and arcuate nuclei—a PCR analysis. *Brain Res Dev Brain Res* 1997; 102:1-12.
 39. Nagao S, Kwak S, Kanazawa I. EAAT4, a glutamate transporter with properties of a chloride channel, is predominantly localized in Purkinje cell dendrites, and forms parasagittal compartments in rat cerebellum. *Neuroscience* 1997; 78:929-33.
 40. Massie A, Vandesande F, Arckens L. Expression of the high-aff-

- finity glutamate transporter EAAT4 in mammalian cerebral cortex. *Neuroreport* 2001; 12:393-7.
41. Fyk-Kolodziej B, Qin P, Dzhagaryan A, Pourcho RG. Differential cellular and subcellular distribution of glutamate transporters in the cat retina. *Vis Neurosci* 2004; 21:551-65.
 42. Pignataro L, Sitaramayya A, Finnemann SC, Sarthy VP. Nonsynaptic localization of the excitatory amino acid transporter 4 in photoreceptors. *Mol Cell Neurosci* 2005; 28:440-51
 43. Arriza JL, Eliasof S, Kavanaugh MP, Amara SG. Excitatory amino acid transporter 5, a retinal glutamate transporter coupled to a chloride conductance. *Proc Natl Acad Sci U S A* 1997; 94:4155-60.
 44. Harvey DM, Calkins DJ. Localization of kainate receptors to the presynaptic active zone of the rod photoreceptor in primate retina. *Vis Neurosci* 2002; 19:681-92.
 45. Calkins DJ. Localization of ionotropic glutamate receptors to invaginating dendrites at the cone synapse in primate retina. *Vis Neurosci* 2005; 22:469-77.
 46. Yang XL. Characterization of receptors for glutamate and GABA in retinal neurons. *Prog Neurobiol* 2004; 73:127-50.
 47. Hughes TE, Hermans-Borgmeyer I, Heinemann S. Differential expression of glutamate receptor genes (GluR1-5) in the rat retina. *Vis Neurosci* 1992; 8:49-55.
 48. Muller F, Greferath U, Wassle H, Wisden W, Seeburg P. Glutamate receptor expression in the rat retina. *Neurosci Lett* 1992; 138:179-82.
 49. Brandstatter JH, Hartveit E, Sassoe-Pognetto M, Wassle H. Expression of NMDA and high-affinity kainate receptor subunit mRNAs in the adult rat retina. *Eur J Neurosci* 1994; 6:1100-12.
 50. Bloomfield SA, Xin D. Surround inhibition of mammalian AII amacrine cells is generated in the proximal retina. *J Physiol* 2000; 523:771-83.
 51. Euler T, Wassle H. Different contributions of GABAA and GABAC receptors to rod and cone bipolar cells in a rat retinal slice preparation. *J Neurophysiol* 1998; 79:1384-95.
 52. Cohen ED, Miller RF. The role of NMDA and non-NMDA excitatory amino acid receptors in the functional organization of primate retinal ganglion cells. *Vis Neurosci* 1994; 11:317-32.
 53. Vardi N. Alpha subunit of Go localizes in the dendritic tips of ON bipolar cells. *J Comp Neurol* 1998; 395:43-52.
 54. Vardi N, Morigiwa K, Wang TL, Shi YJ, Sterling P. Neurochemistry of the mammalian cone 'synaptic complex'. *Vision Res* 1998; 38:1359-69.
 55. Ohia SE, Opere CA, Awe SO, Adams L, Sharif NA. Human, bovine, and rabbit retinal glutamate-induced [3H]D-aspartate release: role in excitotoxicity. *Neurochem Res* 2000; 25:853-60.
 56. Koulen P, Malitschek B, Kuhn R, Wassle H, Brandstatter JH. Group II and group III metabotropic glutamate receptors in the rat retina: distributions and developmental expression patterns. *Eur J Neurosci* 1996; 8:2177-87.
 57. Cai W, Pourcho RG. Localization of metabotropic glutamate receptors mGluR1alpha and mGluR2/3 in the cat retina. *J Comp Neurol* 1999; 407:427-37.
 58. Corti C, Restituito S, Rimland JM, Brabet I, Corsi M, Pin JP, Ferraguti F. Cloning and characterization of alternative mRNA forms for the rat metabotropic glutamate receptors mGluR7 and mGluR8. *Eur J Neurosci* 1998; 10:3629-41.
 59. Koulen P, Brandstatter JH. Pre- and Postsynaptic Sites of Action of mGluR8a in the mammalian retina. *Invest Ophthalmol Vis Sci* 2002; 43:1933-40.
 60. Koulen P. Clustering of neurotransmitter receptors in the mammalian retina. *J Membr Biol* 1999; 171:97-105.
 61. Malherbe P, Kratzeisen C, Lundstrom K, Richards JG, Faull RL, Mutel V. Cloning and functional expression of alternative spliced variants of the human metabotropic glutamate receptor 8. *Brain Res Mol Brain Res* 1999; 67:201-10.
 62. Pow DV, Barnett NL. Developmental expression of excitatory amino acid transporter 5: a photoreceptor and bipolar cell glutamate transporter in rat retina. *Neurosci Lett* 2000; 280:21-4.
 63. Dehnes Y, Chaudhry FA, Ullensvang K, Lehre KP, Storm-Mathisen J, Danbolt NC. The glutamate transporter EAAT4 in rat cerebellar Purkinje cells: a glutamate-gated chloride channel concentrated near the synapse in parts of the dendritic membrane facing astroglia. *J Neurosci* 1998; 18:3606-19.
 64. Fairman WA, Vandenberg RJ, Arriza JL, Kavanaugh MP, Amara SG. An excitatory amino-acid transporter with properties of a ligand-gated chloride channel. *Nature* 1995; 375:599-603.